J. Korean Soc. Ind. Appl. Math. Vol.23, No.2, 65–92, 2019 http://doi.org/10.12941/jksiam.2019.23.065

RECENT DEVELOPMENT OF IMMERSED FEM FOR ELLIPTIC AND ELASTIC INTERFACE PROBLEMS

GWANGHYUN JO [1] AND DO YOUNG KWAK [2]†

[1]DEPARTMENT OF MATHEMATICAL SCIENCES, KAIST, SOUTH KOREA
E-mail address: gwanghyun@kaist.ac.kr

[2] DEPARTMENT OF MATHEMATICAL SCIENCES, KAIST, SOUTH KOREA
E-mail address: kdy@kaist.ac.kr

ABSTRACT. We survey a recently developed immersed finite element method (IFEM) for the interface problems. The IFEM uses structured grids such as uniform grids, even if the interface is a smooth curve. Instead of fitting the curved interface, the bases are modified so that they satisfy the jump conditions along the interface.

The early versions of IFEM [1, 2] were suboptimal in convergence order [3]. Later, the consistency terms were added to the bilinear forms [4, 5], thus the scheme became optimal and the error estimates were proven.

For elasticity problems with interfaces, we modify the Crouzeix-Raviart based element to satisfy the traction conditions along the interface [6], but the consistency terms are not needed. To satisfy the Korn's inequality, we add the stabilizing terms to the bilinear form. The optimal error estimate was shown for a triangular grid.

Lastly, we describe the multigrid algorithms for the discretized system arising from IFEM. The prolongation operators are designed so that the prolongated function satisfy the flux continuity condition along the interface. The $\mathcal{W}$-cycle convergence was proved, and the number of $\mathcal{V}$-cycle is independent of the mesh size.

1. INTRODUCTION

To solve elliptic problems having an interface using finite element methods, it is a common practice to use fitted grid to resolve the smooth interface because unfitted grid yields suboptimal results [7]. However, in recent years, there have been a trend of using unfitted grids for such problems.

Received by the editors April 23 2019; Revised June 8 2019; Accepted in revised form June 10 2019; Published online June 25 2019.

2000 *Mathematics Subject Classification.* 65N30, 74S05, 74B05.

Key words and phrases. immersed finite element method, Crouzeix-Raviart finite element, elasticity problems, heterogeneous materials, traction condition, multigrid method.

† Corresponding author.

First author is supported by National Research Foundation of Korea, grant funded by the Ministry of Education 2019R1I1A1A01055431. Second author is supported by National Research Foundation of Korea, grant funded by the Ministry of Education 2017R1D1A1B03032765.

The purpose of this paper is to give a survey of recent developments in finite element methods for interface problems using unfitted grids. Some of early attempts in this direction are given in the name of XFEM in [8, 9, 10, 11, 12], where they added extra degrees of freedom and/or often used grid refinement near the interface. These methods were mainly designed to resolve crack singularities of solid mechanics problems. Another class of methods, called immersed finite element method(IFE or IFEM) were introduced by Li et al. [1, 2], where they modify the P_1 conforming basis function on unfitted meshes. The modification of basis seems to replace the role of fitting the grids. This method was extended to the case of Crouzeix-Raviart P_1 nonconforming finite element method [13] by Kwak et al. [14].

In early investigation, Li et al. [1, 2] only used modified P_1 conforming basis functions for the same bilinear form as the conventional FEM, and showed the local interpolation error estimate only, assuming high regularity of solutions. By looking at the numerical examples provided by them, the schemes seemed to work for certain cases, but later turned out that the results are suboptimal in general [3]. See [4, 5] where its remedy is suggested. The reason turned out to be that the consistent term errors in the P_1 conforming case cannot be bounded by $O(h)$ when the interface becomes too thin [15]. Thus the consistent terms of the discontinuous Galerkin methods (DG)[16, 17, 18] are needed in the bilinear form. Still, the Crouzeix-Raviart P_1 nonconforming FEM based methods suggested by Kwak et al. [14] work well. Also, the case of nonhomogeneous jumps is considered in [19, 20].

Similar idea was applied to the elasticity problems. Lin et al. [21] have developed a numerical scheme based on P_1/Q_1 conforming finite elements, but it turns out that P_1/Q_1 conforming IFEM basis functions are not uniquely determined for some range of parameters. So they cannot be used to solve elasticity problems in general. Also, the locking phenomena happens as the Lamé constant λ becomes large. Lin et al. [22] have developed an IFEM based on the rotated Q_1 nonconforming element to solve problems with interface, but no analysis is given. Finally, the triangular case with optimal error estimate was given in [6].

The rest of this paper is organized as follows. In section 2, we describe the scalar model problems having interface and define two kinds of schemes (for triangle grids only for simplicity) and show the optimality of the corrected scheme by consistency terms and suboptimality in case of no consistency terms. In section 3, we consider the 2D elasticity problems with modified Crouzeix-Raviart nonconforming basis with stability terms. We show the optimal solvability of the system. In Section 4, we develop the multigrid algorithms for IFEM. We prove the $\mathcal{W}$-cycle convergence and we show that the $\mathcal{V}$-cycle iterations remain bounded as meshsize decreases. In each section, we provide numerical simulations.

2. Scalar Elliptic Problems

Let Ω be a connected, convex polygonal domain in $\mathbb{R}^2$ which is divided into two subdomains Ω^+ and Ω^- by a C^2 interface $\Gamma = \partial\Omega^+ \cap \partial\Omega^-$, see Figure 1. We assume that $\beta(x)$ is a positive function bounded below and above by two positive constants. Although our theory applies to the case of nonconstant $\beta(x)$, we assume $\beta(x)$ is piecewise constant for the simplicity of presentation: there are two positive constants β^+, β^- such that $\beta(x) = \beta^+$ on Ω^+ and $\beta(x) =$

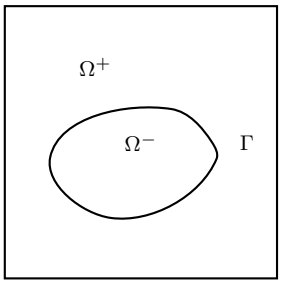

FIGURE 1. A domain Ω with interface

β^- on Ω^-. Consider the following elliptic interface problem

$$-\nabla \cdot (\beta(x)\nabla u) = f \text{ in } \Omega^s \quad (s = +, -) \tag{2.1}$$

$$u = 0 \text{ on } \partial\Omega \tag{2.2}$$

with the jump conditions along the interface

$$[u]_\Gamma = 0, \ \left[\beta(x)\frac{\partial u}{\partial n}\right]_\Gamma = 0, \tag{2.3}$$

where $f \in L^2(\Omega)$ and $u \in H_0^1(\Omega)$ and the bracket $[\cdot]_\Gamma$ means the jump across the interface:

$$[u]_\Gamma := u|_{\Omega^+} - u|_{\Omega^-}.$$

For any domain D, we let $W_p^m(D)$ be the usual Sobolev space with (semi)-norms and denoted by $|\cdot|_{m,p,D}$ and $\|\cdot\|_{m,p,D}$. When $p = 2$, we write $H^m(D) := W_2^m(D)$ with the (semi)-norms $|\cdot|_{m,D}$ and $\|\cdot\|_{m,D}$. Let $H_0^1(\Omega)$ be the subspace of $H^1(\Omega)$ with zero trace on the boundary.

Let $\{\mathcal{T}_h\}$ be the usual shape regular triangulations of the domain Ω by the triangles of maximum diameter h which may not be aligned with the interface Γ. For each $T \in \mathcal{T}_h$, let

$$\widetilde{W}_p^m(T) := \{\, u \in L^2(T) : \, u|_{T\cap\Omega^s} \in W_p^m(T \cap \Omega^s), s = +, - \,\}, \ p \geq 1, \ m \geq 0$$

with norms;

$$|u|_{m,p,T}^2 := |u|_{m,p,T\cap\Omega^+}^2 + |u|_{m,p,T\cap\Omega^-}^2,$$
$$\|u\|_{m,p,T}^2 := \|u\|_{m,p,T\cap\Omega^+}^2 + \|u\|_{m,p,T\cap\Omega^-}^2.$$

Now we define $\widetilde{W}_p^m(\Omega)$ to be the space of all functions $u \in L^2(\Omega)$ such that $u|_T \in \widetilde{W}_p^m(T)$ for all $T \in \mathcal{T}_h$ equipped with the broken (semi)-norms $|u|_{\widetilde{W}_p^m(\Omega)} := \left(\sum_T |u|_{m,p,T}^2\right)^{1/2}$ and $\|u\|_{\widetilde{W}_p^m(\Omega)} := \left(\sum_T \|u\|_{m,p,T}^2\right)^{1/2}$. When $p = 2$, we write $\widetilde{H}^m(D) = \widetilde{W}_p^m(D)$ for $D = T, \Omega$

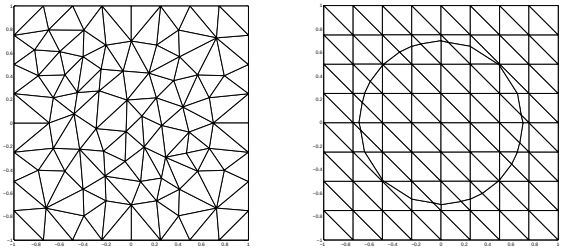

(a) Fitted grid (b) Uniform Grid

and denote their (semi)-norms by $|u|_{\widetilde{H}^m(D)}$ and $\|u\|_{\widetilde{H}^m(D)}$. We also need some subspaces of $\widetilde{H}^2(T)$ and $\widetilde{H}^2(\Omega)$ satisfying the jump conditions:

$$\widetilde{H}^2_\Gamma(T) := \left\{ u \in H^1(T) : u|_{T\cap\Omega^s} \in H^2(T\cap\Omega^s),\ s=+,-,\ \left[\beta\frac{\partial u}{\partial n}\right]_\Gamma = 0 \text{ on } \Gamma\cap T \right\}$$

$$\widetilde{H}^2_\Gamma(\Omega) := \{ u \in H^1_0(\Omega) : u|_T \in \widetilde{H}^2_\Gamma(T),\ \forall T \in \mathcal{T}_h\}.$$

Throughout the paper, the constants C, C_0, C_1, etc., are generic constants independent of the mesh size h and functions u, v but may depend on the problem data β, f and Ω, and are not necessarily the same on each occurrence.

The usual weak formulation for the problem (2.1) - (2.3) is: Find $u \in H^1_0(\Omega)$ such that

$$\int_\Omega \beta(x)\nabla u\cdot\nabla v dx = \int_\Omega fv dx,\ \forall v \in H^1_0(\Omega). \tag{2.4}$$

We have the following existence theorem for this problem [23, 24].

Theorem 2.1. *Assume that $f \in L^2(\Omega)$. Then the variational problem (2.4) has a unique solution $u \in \widetilde{H}^2(\Omega)$ which satisfies*

$$\|u\|_{\widetilde{H}^2(\Omega)} \le C\|f\|_{L^2(\Omega)}.$$

2.1. **P_1-immersed finite element methods.** We briefly review the immersed finite element space based on the P_1 - Lagrange basis functions ([1, 2]). Let $\{\mathcal{T}_h\}$ be the usual quasi-uniform finite element triangulations of the domain Ω. We call an element $T \in \mathcal{T}_h$ an *interface element* if the interface Γ passes through the interior of T, otherwise we call it a *noninterface* element. Let $\mathcal{T}_h^I$ be the collection of all interface elements. We assume that the interface meets the edges of an interface element at no more than two points.

We construct the local basis functions on each element T of the partition $\mathcal{T}_h$. For a noninterface element $T \in \mathcal{T}_h$, we simply use the standard linear shape functions on T whose degrees of freedom are functional values on the vertices of T, and use $S_h(T)$ to denote the linear spaces spanned by the three nodal basis functions on T:

$$S_h(T) = \text{span}\{\ \phi_i\ :\ \phi_i \text{ is the standard linear shape function }\}$$

We let $S_h(\Omega)$ denote the space of usual continuous, piecewise linear polynomials with vanishing boundary values.

Now we consider a typical interface element $T \in \mathcal{T}_h^I$ whose geometric configuration is given as in Fig. 2. Here the curve between the two points D and E is a part of the interface and $\overline{DE}$ is the line segment connecting the intersections of the interface and the edges.

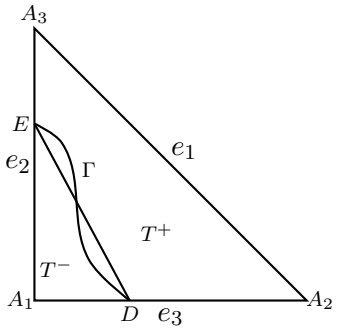

FIGURE 2. A typical interface triangle

We construct piecewise linear basis functions $\hat{\phi}_i, i = 1, 2, 3$ of the form

$$\hat{\phi}_i(X) = \begin{cases} a^+ + b^+x + c^+y, & X = (x, y) \in T^+, \\ a^- + b^-x + c^-y, & X = (x, y) \in T^-, \end{cases}$$

satisfying

$$\begin{aligned} \hat{\phi}_i(A_j) &= \delta_{ij},\ j = 1, 2, 3, \\ [\hat{\phi}_i(D)] &= [\hat{\phi}_i(E)] = 0, \\ \left[\beta \frac{\partial \hat{\phi}_i}{\partial \mathbf{n}}\right]_{\overline{DE}} &= 0. \end{aligned}$$

These are continuous, piecewise linear functions on T satisfying the flux jump condition along $\overline{DE}$, whose uniqueness and existence are known [15, 1]. We denote by $\widehat{S}_h(T)$ the space of functions generated by $\hat{\phi}_i$, $i = 1, 2, 3$ constructed above. Next we define the global *immersed finite element space* $\widehat{S}_h(\Omega)$ to be the set of all functions $\phi \in L^2(\Omega)$ such that

$$\left\{ \begin{array}{l} \phi \in \widehat{S}_h(T) \text{ if } T \in \mathcal{T}_h^I, \text{ and } \phi \in S_h(T) \text{ if } T \notin \mathcal{T}_h^I, \\ \text{having continuity at all vertices of the triangulation} \\ \text{and vanishes on the boundary vertices.} \end{array} \right\}$$

We note that a function in $\widehat{S}_h(\Omega)$, in general, is not continuous across an edge common to two interface elements. Let $H_h(\Omega) := H_0^1(\Omega) + \widehat{S}_h(\Omega)$ and equip it with the piecewise norms $|u|_{1,h} := |u|_{\widetilde{H}^1(\Omega)}$, $\|u\|_{1,h} := \|u\|_{\widetilde{H}^1(\Omega)}$. Next, we define the interpolation operator. For any $u \in \widetilde{H}_\Gamma^2(T)$, we let $\hat{I}_h u \in \widehat{S}_h(T)$ be such that

$$\hat{I}_h u(A_i) = u(A_i),\ i = 1, 2, 3,$$

where A_i, $i = 1, 2, 3$ are the vertices of T and we call $\hat{I}_h u$ the local *interpolant* of u in $\widehat{S}_h(T)$. We naturally extend it to $\widetilde{H}^2_\Gamma(\Omega)$ by $(\hat{I}_h u)|_T = \hat{I}_h(u|_T)$ for each T. Then we have the following approximation property [14, 2].

Proposition 2.1. *There exists a constant $C > 0$ such that*

$$\sum_{T\in\mathcal{T}_h} (\|u - \hat{I}_h u\|_{0,T} + h|u - \hat{I}_h u|_{1,T}) \le Ch^2 \|u\|_{\widetilde{H}^2(\Omega)}$$

for all $u \in \widetilde{H}^2_\Gamma(\Omega)$.

Now the IFEM based on the P_1- Lagrange basis functions introduced in [1, 2] reads:
(P_1-IFEM) Find $u_h \in \widehat{S}_h(\Omega)$ such that

$$a_h(u_h, v_h) = (f, v_h),\ \forall\, v_h \in \widehat{S}_h(\Omega),$$

where

$$a_h(u, v) = \sum_{T\in\mathcal{T}_h} \int_T \beta \nabla u \cdot \nabla v\, dx,\ \forall\, u, v \in H_h(\Omega).$$

As it turns out later in [3], this scheme is suboptimal, see [4]. Hence we need a modified scheme by adding consistency terms.

2.2. **Modified P_1-IFEM.** In this section, we modify the P_1-IFEM above by adding the line integrals for jumps of fluxes and functional values. The method resembles the discontinuous Galerkin methods (see [17, 25] and references therein) which use completely discontinuous basis functions, but the degrees of freedom in our method are much smaller than the DG methods since this method has the same number of basis functions as the conventional P_1-FEM.

In order to describe this modified method, we need some additional notations. Let the collection of all the edges of $T \in \mathcal{T}_h$ be denoted by $\mathcal{E}_h$ and we split $\mathcal{E}_h$ into two disjoint sets; $\mathcal{E}_h = \mathcal{E}_h^o \cup \mathcal{E}_h^b$, where $\mathcal{E}_h^o$ is the set of edges lying in the interior of Ω, and $\mathcal{E}_h^b$ is the set of edges on the boundary of Ω. In particular, we denote the set of edges cut by the interface Γ by $\mathcal{E}_h^I$. For every $e \in \mathcal{E}_h^o$, there are two element T_1 and T_2 sharing e as a common edge. Let $\mathbf{n}_{T_i}, i = 1, 2$ be the unit outward normal vector to the boundary of T_i, but for the edge e, we choose a direction of the normal vector, say $\mathbf{n}_e = \mathbf{n}_{T_1}$ and fix it once and for all. For functions v defined on $T_1 \cup T_2$, we let $[\cdot]_e$ and $\{\cdot\}_e$ denote the jump and average across e respectively, i.e.

$$\{v\}_e(x) := \frac{1}{2} \lim_{\delta\to 0+} \left(v(x - \delta\mathbf{n}_e) + v(x + \delta\mathbf{n}_e)\right),$$
$$[v]_e(x) := \lim_{\delta\to 0+} \left(v(x - \delta\mathbf{n}_e) - v(x + \delta\mathbf{n}_e)\right).$$

We also need the mesh dependent norm $|\!|\!| \cdot |\!|\!|$ on the space $H_h(\Omega)$,

$$|\!|\!| v |\!|\!|^2 := \sum_{T\in\mathcal{T}_h} \|v\|^2_{0,T} + \sum_{T\in\mathcal{T}_h} \|\nabla v\|^2_{0,T} + \sum_{e\in\mathcal{E}_h^o} h \left\| \left\{ \frac{\partial v}{\partial \mathbf{n}_e} \right\}_e \right\|^2_{0,e} + \sum_{e\in\mathcal{E}_h^o} h^{-1} \|[v]\|^2_{0,e}.$$

Multiplying both sides of the equation (2.1) by $v \in H^1(T)$, applying Green's formula and adding terms, we get

$$\sum_{T\in\mathcal{T}_h}\left(\int_T \beta\nabla u\cdot\nabla v dx - \int_{\partial T}\beta\nabla u\cdot\mathbf{n}_T\, v ds\right) = \int_\Omega f v dx.$$

By using the preassigned normal vectors $\mathbf{n}_e$ and adding the unharmful term $\epsilon\int_e\{\beta\nabla v\cdot\mathbf{n}_e\}_e[u]_e ds$ for any ϵ, we see the left hand side of above equation becomes

$$\sum_{T\in\mathcal{T}_h}\int_T \beta\nabla u\ \cdot\ \nabla v dx\ -\ \sum_{e\in\mathcal{E}_h^o}\int_e\{\beta\nabla u\ \cdot\ \mathbf{n}_e\}_e[v]_e ds\ +\ \epsilon\sum_{e\in\mathcal{E}_h^o}\int_e\{\beta\nabla v\ \cdot\ \mathbf{n}_e\}_e[u]_e ds$$

which is valid for $v\in L^2(\Omega)\cap H^1(T)$ for all $T\in\mathcal{T}_h$. We define the following bilinear forms

$$\begin{aligned}
b_\epsilon(u,v) &:= -\sum_{e\in\mathcal{E}_h^o}\int_e\{\beta\nabla u\cdot\mathbf{n}\}_e[v]_e ds, +\epsilon\sum_{e\in\mathcal{E}_h^o}\int_e\{\beta\nabla v\cdot\mathbf{n}\}_e[u]_e ds,\\
j_\sigma(u,v) &:= \sum_{e\in\mathcal{E}_h^o}\int_e\frac{\sigma}{h}[u]_e[v]_e ds,\ \text{for some } \sigma>0,\\
a_\epsilon(u,v) &:= a_h(u,v)+b_\epsilon(u,v)+j_\sigma(u,v).
\end{aligned}$$

Now, for each $\epsilon=0$, $\epsilon=-1$ and $\epsilon=1$, we define the modified P_1-IFEM for the problem (2.1)-(2.3):

(Modified P_1-IFEM) Find $u_h^m\in\widehat{S}_h(\Omega)$ such that

$$a_\epsilon(u_h^m,v_h)=(f,v_h),\ \forall v_h\in\widehat{S}_h(\Omega). \tag{2.5}$$

This is similar to a class of DG methods, corresponding to IP, SIPG, NIPG and OBB ([16, 25, 18, 26]), if $\epsilon=0$, $\epsilon=-1$, $\epsilon=1$, and $\epsilon=0,\sigma=0$, respectively.

The following result is given in [4, 5].

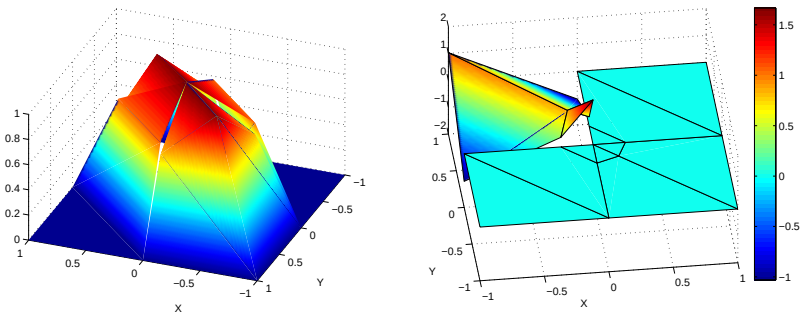

FIGURE 3. Lagrange vs Crouzeix-Raviart basis

Theorem 2.2. *Let u be the solution of (2.1)-(2.3) and let u_h be the solution of (2.5). Then $\exists$ const $C_0 > 0$ such that*

$$\|\!|u - u_h|\!\| \leq C_0 h \|u\|_{\widetilde{H}^2(\Omega)}.$$

2.3. **Crouzeix-Raviart P_1 nonconforming finite element.** We now consider a IFEM based on Crouzeix-Raviart P_1 nonconforming finite element. i.e. the degrees of freedom is the edge averages. For this presentation we slightly change notation. The problem we consider is

$$-\nabla \cdot (\beta(x)\nabla p) = f \text{ in } \Omega^s \quad (s = +, -) \tag{2.6}$$

$$p = 0 \text{ on } \partial\Omega \tag{2.7}$$

with the jump conditions along the interface

$$[p]_\Gamma = 0, \ \left[\beta(x)\frac{\partial p}{\partial n}\right]_\Gamma = 0. \tag{2.8}$$

Geometric configuration of a typical reference interface element T is given in Fig. 2 in which the curve between points D and E is part of the interface. Let e_i, $i = 1, 2, 3$ be the edges of T. For $\phi \in H^1(T)$, let $\bar{\phi}_{e_i}$ denote the average of ϕ along e_i, i.e., $\bar{\phi}_{e_i} := \frac{1}{|e_i|}\int_{e_i} \phi \, ds$.

We construct a piecewise linear function of the form

$$\phi(X) = \begin{cases} \phi^+(X) = a_0 + b_0 x + c_0 y, & X = (x, y) \in T^+, \\ \phi^-(X) = a_1 + b_1 x + c_1 y, & X = (x, y) \in T^-, \end{cases} \tag{2.9}$$

satisfying

$$\bar{\phi}_{e_i} = V_i, \ i = 1, 2, 3, \tag{2.10}$$

$$\phi^+(D) = \phi^-(D), \ \phi^+(E) = \phi^-(E), \ \overline{\beta^+}\frac{\partial \phi^+}{\partial \mathbf{n}_{\overline{DE}}} = \overline{\beta^-}\frac{\partial \phi^-}{\partial \mathbf{n}_{\overline{DE}}}, \tag{2.11}$$

where V_i, $i = 1, 2, 3$ are given values, $\mathbf{n}_{\overline{DE}}$ is the unit normal vector on the line segment $\overline{DE}$, and $\overline{\beta^+}$, $\overline{\beta^-}$ are averages along $\overline{DE}$. This is a piecewise linear function on T that satisfies the homogeneous jump conditions along $\overline{DE}$.

Theorem 2.3. *Given a reference interface triangle, the piecewise linear function $\phi(x, y)$ defined by (2.9)-(2.11) is uniquely determined.*

Now we can construct nodal basis functions on an interface element T in general position through affine mapping. We let $\widehat{N}_h(T)$ to denote the three-dimensional linear space spanned by these shape functions. We note that $\widehat{N}_h(T)$ is a subspace of $H^1(T)$. When no interface is involved, we use the notation $N_h(T)$ for $\widehat{N}_h(T)$. Finally, we define the *immersed finite element*

space $\widehat{N}_h(\Omega)$ as the collection of functions such that

$$\begin{cases} \phi|_T \in N_h(T), \text{ if } T \text{ is a noninterface element,} \\ \phi|_T \in \widehat{N}_h(T), \text{ if } T \text{ is an interface element,} \\ \displaystyle\int_e \phi|_{T_1}\, ds = \int_e \phi|_{T_2}\, ds, \text{ if } T_1,\, T_2 \text{ are adjacent elements and } e \text{ is a common edge of } T_1 \text{ and } T_2, \\ \displaystyle\int_e \phi\, ds = 0, \text{ if } e \text{ is part of the boundary } \partial\Omega. \end{cases}$$

2.4. **Approximation property of nonconforming immersed space $\widehat{N}_h(T)$.** In this subsection, we would like to study the approximation property of $\widehat{N}_h(T)$ by defining an interpolation operator. The difficulty lies in the fact that $\widehat{N}_h(T)$ does not belong to $\widetilde{H}^2(T)$, the restriction of $\widetilde{H}^2(\Omega)$ on T, where $\widetilde{H}^2(T) = H^1(T) \cap H^2(T \cap \Omega^+) \cap H^2(T \cap \Omega^-)$(see Fig. 4). To overcome the difficulty, we introduce a bigger space which contains both of these spaces.

For a given interface element T, we consider a function space $X(T)$ such that every $p \in X(T)$ satisfies

$$\begin{cases} p \in H^1(T) \cap H^2(T^+ \cap \Omega^+) \cap H^2(T^- \cap \Omega^-) \cap H^2(T_r^+) \cap H^2(T_r^-), \\ \displaystyle\int_{\Gamma \cap T} (\beta^- \operatorname{grad} p^- - \beta^+ \operatorname{grad} p^+) \cdot \mathbf{n}_\Gamma\, ds = 0, \end{cases}$$

where $T_r = T - (\Omega^+ \cap T^+) - (\Omega^- \cap T^-)$ and $T_r^s = T_r \cap \Omega^s,\ s = +, -$. For any $p \in X(T)$, we define the following norms.

$$\begin{aligned} |p|^2_{X(T)} &= |p|^2_{2,T^- \cap \Omega^-} + |p|^2_{2,T^+ \cap \Omega^+} + |p|^2_{2,T_r^-} + |p|^2_{2,T_r^+}, \\ \|p\|^2_{X(T)} &= \|p\|^2_{1,T} + |p|^2_{X(T)}, \\ |\!|\!| p |\!|\!|_{2,T} &= |p|_{X(T)} + \sum_{i=1}^{3} |\bar{p}_{e_i}|, \end{aligned}$$

where $\bar{p}_{e_i},\ i = 1, 2, 3$ are the average on each edge e_i. Then we have [14]

Lemma 2.2. *Let T be an interface element. Then for any $p \in X(T)$, we have*

$$\|p - I_h p\|_{m,T} \le C h^{2-m} \|p\|_{X(T)},\ m = 0, 1,$$

where h is the mesh size of T.

Now the **CR based IFEM** is simply : Find $p_h \in \widehat{N}_h(\Omega)$ such that

$$a_h(p_h, q_h) = (f, q_h),\ \forall\, q_h \in \widehat{N}_h(\Omega), \tag{2.12}$$

where

$$a_h(p, q) = \sum_{T \in \mathcal{T}_h} \int_T \beta \nabla p \cdot \nabla q\, dx,\ \forall\, p, q \in H_h(\Omega) \equiv H(\Omega) + \widehat{N}_h(\Omega).$$

Lemma 2.3 (Second Strang Lemma)**.** *If $p \in \widetilde{H}^2(\Omega)$, $p_h \in \widehat{N}_h(\Omega)$ are the solutions of (2.6) and (2.12) respectively, then there exists a constant $C > 0$ such that*

$$\|p - p_h\|_{1,h} \leq C \left\{ \inf_{q_h \in \widehat{N}_h(\Omega)} \|p - q_h\|_{1,h} + \sup_{\phi_h \in \widehat{N}_h(\Omega)} \frac{|\, a_h(p, \phi_h) - (f, \phi_h)\,|}{\|\phi_h\|_{1,h}} \right\}.$$

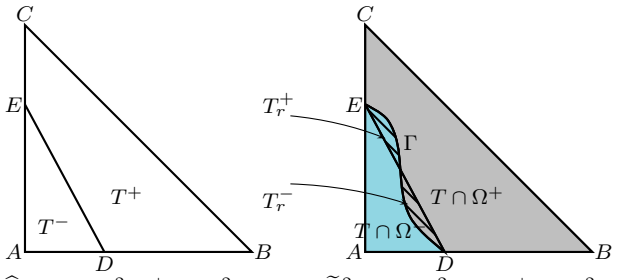

(a) $\widehat{N}_h(T) \subset H^2(T^+) \cap H^2(T^-)$ (b) $\widetilde{H}^2(T) \subset H^2(T \cap \Omega^+) \cap H^2(T \cap \Omega^-)$

FIGURE 4. The real interface and the approximated interface

Using Lemma 2.2 and 2.3, we obtain

Theorem 2.4. [14] *Let p be the solution of (2.6)-(2.8) and let p_h be the IFEM solution. Then there exists a positive constant C_0 such that*

$$|\!|\!| p - p_h |\!|\!| \quad \leq \quad C_0 h \|p\|_{\widetilde{H}^2(\Omega)}.$$

The L^2-error estimate easily follows from the duality technique.

Theorem 2.5. *The solution p_h satisfies*

$$\|p - p_h\|_{0,\Omega} \quad \leq \quad C h^2 \|p\|_{\widetilde{H}^2(\Omega)}.$$

2.5. **Mixed finite volume method based on IFEM.** In this section, we propose a new mixed finite volume method based on the 'broken' P_1-nonconforming finite element method introduced in the previous section. Our method is similar to the mixed finite volume method studied in [27, 28, 29], but the usual nonconforming finite element space is replaced by our 'broken' P_1-nonconforming space.

Let us write the problem (2.6) in a mixed form by introducing the vector variable $\mathbf{u} = -\beta \operatorname{grad} p$ as

$$\left\{ \begin{array}{rl} \mathbf{u} + \beta \operatorname{grad} p = 0 & \text{in } \Omega, \\ \operatorname{div} \mathbf{u} = f & \text{in } \Omega, \\ p = 0 & \text{on } \partial\Omega. \end{array} \right. \tag{2.13}$$

The mixed finite element method based on this dual formulation is well-known [30, 31, 32]. In the mixed method, we need to find a direct approximation of the flow variable $\mathbf{u}$. For that purpose, we introduce $\mathbf{V} = \mathbf{H}(\operatorname{div}, \Omega) = \{\mathbf{v} \in \mathbf{L}^2(\Omega) : \operatorname{div} \mathbf{v} \in L^2(\Omega)\}$, and use the

local RT_0 space to approximate the flow variable which is given by $\mathbf{V}_h(T) = \{v \,:\, v = (a+cx, b+cy),\ a,b,c \in \mathbb{R}\}$ for any triangular element T. The global space $\mathbf{V}_h$ is defined as

$$\mathbf{V}_h = \{\mathbf{v} \,:\, \mathbf{v}|_T \in \mathbf{V}_h(T);\ \mathbf{v}\cdot\mathbf{n} \text{ is continuous along interior edges}\}.$$

This method gives a good approximation of the flow variable. However, it leads to a saddle point problem, that is, one obtains an indefinite matrix system when (2.13) is discretized. As mentioned earlier, a popular way to avoid this indefinite system is to use Lagrange multipliers [33]. Another possibility is to form a mixed finite volume method as in [27, 28, 29].

To define a mixed finite volume method for an interface problem, we use the well-known RT_0 space $\mathbf{V}_h$ for velocity and 'broken' P_1-nonconforming immersed space $\widehat{N}_h$ for pressure variable. Note that every $\mathbf{v} \in \mathbf{V}_h$ has continuous normal components across the edges of $\mathcal{T}_h$, which are constant.

We consider the following scheme: Find $(\mathbf{u}_h, p_h) \in \mathbf{V}_h \times \widehat{N}_h$ which satisfies on each element $T \in \mathcal{T}_h$

$$\begin{cases} \displaystyle\int_T (\mathbf{u}_h + \beta\,\mathrm{grad}\, p_h)\cdot\ \mathrm{grad}\,\phi = 0, \quad \forall \phi \in \widehat{N}_h(T), \\ \displaystyle\int_T \mathrm{div}\mathbf{u}_h = \int_T f. \end{cases} \tag{2.14}$$

Note that since $\mathrm{div}\mathbf{u}_h$ is constant, $\mathrm{div}\mathbf{u}_h|_T = \overline{f}|_T := \frac{1}{|T|}\int_T f$, where $|T|$ denotes the area of T, which implies

$$\int_T \mathrm{div}\mathbf{u}_h|_T \phi = \int_T \overline{f}|_T \phi, \quad \phi \in \widehat{N}_h(T).$$

When the interface is not present, $\widehat{N}_h(T) = N_h(T)$ and this scheme coincides with the one in [27, 29]. Since the numbers of unknowns and equations do not change, our scheme is a square linear system and has a unique solution. We refer to [27] for details.

Now since $\mathbf{u}_h\cdot\mathbf{n}$ is constant on the edge and $\phi \in \widehat{N}_h$ has common average values on interior edges and vanishing boundary nodal values, we obtain

$$\sum_{T\in\mathcal{T}_h}\int_T \mathbf{u}_h\cdot\ \mathrm{grad}\,\phi \;=\; \sum_{T\in\mathcal{T}_h}\left[\int_{\partial T}(\mathbf{u}_h\cdot\mathbf{n})\phi - \int_T \mathrm{div}\mathbf{u}_h\phi\right] = -\int_\Omega \overline{f}\phi,$$

From (2.14), it immediately follows that

$$\sum_{T\in\mathcal{T}_h}\int_T \beta\,\mathrm{grad}\, p_h\cdot\ \mathrm{grad}\,\phi \;=\; \int_\Omega \overline{f}\phi,\ \forall\phi\in\widehat{N}_h(\Omega). \tag{2.15}$$

This is exactly the same as the immersed finite element method introduced in the previous section, except that on the right-hand side f is replaced by $\overline{f}$. The velocity $\mathbf{u}_h$ can be computed directly from the solution p_h of (2.15) as follows. Let T be an element of $\mathcal{T}_h$ with the edges $e_i,\ i=1,2,3$ and let $\phi_i \in \widehat{N}_h(T)$ be the 'broken' P_1-nonconforming basis function associated

with the edge e_i. Then the flux through the edge e_i is given by

$$\begin{aligned} |e_i|(\mathbf{u}_h \cdot \mathbf{n})|_{e_i} &= \int_{\partial T} (\mathbf{u}_h \cdot \mathbf{n})\phi_i = \int_T \mathrm{div}(\mathbf{u}_h \phi_i) \\ &= \int_T (\mathrm{div}\mathbf{u}_h \phi_i + \mathbf{u}_h \cdot \mathrm{grad}\, \phi_i), \end{aligned}$$

where $\phi_i \in \widehat{N}_h(T)$ is a basis function on T. Then it follows by (2.14) that

$$|e_i|(\mathbf{u}_h \cdot \mathbf{n})|_{e_i} = \int_T \overline{f}\phi_i - \int_T \beta\, \mathrm{grad}\, p_h \cdot \mathrm{grad}\, \phi_i.$$

Thus in order to compute the fluxes through the edges of an element T, we only need to compute the local residual of the solution p_h on each T.

The error estimate of $\mathbf{u}_h$ would follow that of p_h. In fact, we can relate the estimate $\|\mathbf{u} - \mathbf{u}_h\|_0$ with $\|p - p_h\|_{1,h}$. First, we show the following local formula.

Lemma 2.4. *Let $\mathbf{u}_h$, p_h be the solutions of (2.14), then*

$$\mathbf{u}_h(\mathbf{x}) = -\overline{\beta\, grad\, p_h} + \frac{\overline{f}}{2}(\mathbf{x} - \mathbf{x}_B),\ \forall \mathbf{x} \in T,$$

where $\overline{\beta\, grad\, p_h}$ denotes the average of $\beta\, grad\, p_h$ on T and $\mathbf{x}_B$ is the center of T.

Using the above lemma, we can show

Theorem 2.6. *Let $\mathbf{u}_h$, p_h be the solutions of (2.14), then there exists a constant $C > 0$ such that*

$$\|\mathbf{u} - \mathbf{u}_h\|_{L^2(\Omega)} + \|\mathrm{div}\mathbf{u} - \mathrm{div}\mathbf{u}_h\|_{L^2(\Omega)} \le Ch \left\{ \|\mathbf{u}\|_{\mathbf{H}^1(\Omega)} + \|p\|_{\widetilde{H}^2(\Omega)} + \|f\|_{\tilde{H}^1(\Omega)} \right\},$$

provided $\mathbf{u} \in \mathbf{H}^1(\Omega)$.

2.6. **Numerical experiment for CR- based IFEM and Mixed IFEM.**

Example 2.5. *Take a circle with radius $r_0 = 0.5$ as an interface, and choose the exact solution*

$$p = \begin{cases} \dfrac{r^3}{\beta^-} & \text{in } \Omega^-, \\ \dfrac{r^3}{\beta^+} + (\dfrac{1}{\beta^-} - \dfrac{1}{\beta^+})r_0^3 & \text{in } \Omega^+. \end{cases}$$

In this example, two cases $\beta^+/\beta^- = 1/1000$ and $\beta^+/\beta^- = 1000$ are reported in Tables 1 and 2.

Example 2.6 (Variable coefficient)**.** *We take the level set of $L = x^2/(0.5)^2 + y^2/(0.25)^2 - 1.0$ as an interface. The exact solution is chosen as $p = L(x, y)/\beta$ where*

$$\beta = \begin{cases} 1 + 0.5(x^2 - xy + y^2) & \text{on } \Omega^-, \\ 1 & \text{on } \Omega^+. \end{cases}$$

$1/h$	$\|p-p_h\|_0$	*order*	$\|p-p_h\|_{1,h}$	*order*	$\|\mathbf{u}-\mathbf{u}_h\|_0$	*order*	$\|\mathrm{div}(\mathbf{u}-\mathbf{u}_h)\|_0$	*order*
8	*9.576e-3*		*1.208e-1*		*2.945e-1*		*1.053e+0*	
16	*2.666e-3*	*1.845*	*6.744e-2*	*0.841*	*1.702e-1*	*0.791*	*5.292e-1*	*0.993*
32	*6.488e-4*	*2.039*	*3.341e-2*	*1.013*	*8.906e-2*	*0.934*	*2.650e-1*	*0.998*
64	*1.400e-4*	*2.212*	*1.657e-2*	*1.012*	*4.290e-2*	*1.054*	*1.326e-1*	*0.999*
128	*3.716e-5*	*1.914*	*8.242e-3*	*1.008*	*2.015e-2*	*1.090*	*6.629e-2*	*1.000*
256	*8.973e-6*	*2.050*	*4.117e-3*	*1.001*	*9.865e-3*	*1.030*	*3.315e-2*	*1.000*
Order		*2.029*		*0.985*		*0.994*		*0.998*

TABLE 1. Nonconforming immersed FEM: $\beta^- = 1, \beta^+ = 1000$

$1/h$	$\|p-p_h\|_0$	*order*	$\|p-p_h\|_{1,h}$	*order*	$\|\mathbf{u}-\mathbf{u}_h\|_0$	*order*	$\|\mathrm{div}(\mathbf{u}-\mathbf{u}_h)\|_0$	*order*
8	*1.447e-2*		*6.575e-1*		*3.361e-1*		*1.053e+0*	
16	*3.497e-3*	*2.049*	*3.312e-1*	*0.989*	*1.657e-1*	*1.020*	*5.292e-1*	*0.993*
32	*8.826e-4*	*1.986*	*1.661e-1*	*0.996*	*8.165e-2*	*1.021*	*2.650e-1*	*0.998*
64	*2.210e-4*	*1.998*	*8.311e-2*	*0.999*	*4.075e-2*	*1.003*	*1.326e-1*	*0.999*
128	*5.507e-5*	*2.005*	*4.157e-2*	*0.999*	*1.959e-2*	*1.057*	*6.629e-2*	*1.000*
256	*1.370e-5*	*2.007*	*2.079e-2*	*1.000*	*9.658e-3*	*1.020*	*3.315e-2*	*1.000*
Order		*2.005*		*0.997*		*1.024*		*0.998*

TABLE 2. Nonconforming immersed FEM: $\beta^- = 1000, \beta^+ = 1$

It can be easily checked that this solution indeed satisfies the jump condition. The results are reported in Table 3.

$1/h$	$\|p-p_h\|_0$	*order*	$\|p-p_h\|_{1,h}$	*order*	$\|\mathbf{u}-\mathbf{u}_h\|_0$	*order*	$\|\mathrm{div}(\mathbf{u}-\mathbf{u}_h)\|_0$	*order*
8	*2.877e-1*		*4.742e+0*		*3.398e+0*		*5.499e-1*	
16	*7.343e-2*	*1.970*	*2.386e+0*	*0.991*	*1.722e+0*	*0.980*	*3.802e-1*	*0.532*
32	*1.842e-2*	*1.995*	*1.195e+0*	*0.997*	*8.646e-1*	*0.994*	*1.908e-1*	*0.995*
64	*4.608e-3*	*1.999*	*5.981e-1*	*0.999*	*4.328e-1*	*0.998*	*8.894e-2*	*1.101*
128	*1.152e-3*	*2.000*	*2.991e-1*	*1.000*	*2.165e-1*	*0.999*	*4.409e-2*	*1.012*
256	*2.881e-4*	*2.000*	*1.495e-1*	*1.000*	*1.083e-1*	*1.000*	*2.208e-2*	*0.998*
Order		*1.993*		*0.997*		*0.994*		*0.928*

TABLE 3. Nonconforming immersed FEM: $\beta^- = 1 + 0.5(x^2 - xy + y^2), \beta^+ = 1$

Example 2.7 (Sharp Edge)**.** *In this example, we consider an interface with sharp edge. With* $L = -y^2 + ((x-1)\tan\theta)^2 x$*, the level set has a sharp corner of angle* 2θ *at the point* $(1,0)$*(see Figure 5. The exact solution is chosen as* $p = L(x,y)/\beta$ *where* $\beta^- = 1, \beta^+ = 1000$*. We have tested two cases:* $\theta = 10^o$*,* $\theta = 40^o$ *and the results are reported in Tables 4 and 5.*

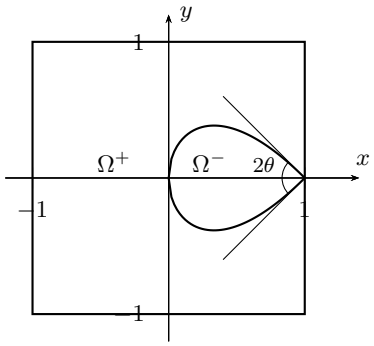

FIGURE 5. Level set of $y^2 = ((x-1)\tan\theta)^2 x$

$1/h$	$\|p-p_h\|_0$	*order*	$\|p-p_h\|_{1,h}$	*order*	$\|\mathbf{u}-\mathbf{u}_h\|_0$	*order*	$\|\mathrm{div}(\mathbf{u}-\mathbf{u}_h)\|_0$	*order*
8	*2.058e-2*		*3.164e-1*		*2.709.e-1*		*2.195e-2*	
16	*5.349e-3*	*1.944*	*1.605e-1*	*0.979*	*1.381e-1*	*0.972*	*1.096e-2*	*1.001*
32	*1.422e-3*	*1.911*	*8.010e-2*	*1.003*	*7.263e-2*	*0.927*	*5.489e-3*	*0.998*
64	*3.564e-4*	*1.997*	*4.021e-2*	*0.994*	*4.158e-2*	*0.805*	*2.746e-3*	*0.999*
128	*8.756e-5*	*2.025*	*2.004e-2*	*1.005*	*1.938e-2*	*1.101*	*1.373e-3*	*1.000*
256	*2.164e-5*	*2.017*	*9.999e-3*	*1.003*	*9.192e-3*	*1.076*	*6.868e-4*	*1.000*
Order		*1.979*		*0.997*		*0.976*		*1.000*

TABLE 4. Nonconforming immersed FEM -Sharp Edge, $\theta = 10^o$: $\beta^- = 1, \beta^+ = 1000$

$1/h$	$\|p-p_h\|_0$	*order*	$\|p-p_h\|_{1,h}$	*order*	$\|\mathbf{u}-\mathbf{u}_h\|_0$	*order*	$\|\mathrm{div}(\mathbf{u}-\mathbf{u}_h)\|_0$	*order*
8	*1.380e-2*		*1.677e-1*		*5.366e-1*		*4.902e-1*	
16	*3.753e-3*	*1.878*	*9.986e-2*	*0.748*	*2.167e-1*	*1.308*	*2.471e-1*	*0.988*
32	*8.606e-4*	*2.124*	*3.811e-2*	*1.390*	*1.060e-1*	*1.031*	*1.240e-1*	*0.994*
64	*2.192e-4*	*1.973*	*1.544e-2*	*1.303*	*5.117e-2*	*1.051*	*6.211e-2*	*0.998*
128	*5.567e-5*	*1.977*	*7.339e-3*	*1.073*	*2.451e-2*	*1.062*	*3.108e-2*	*0.999*
256	*1.359e-5*	*2.034*	*3.510e-3*	*1.064*	*1.196e-2*	*1.035*	*1.555e-2*	*0.999*
Order		*1.997*		*1.116*		*1.097*		*0.996*

TABLE 5. Nonconforming immersed FEM -Sharp Edge, $\theta = 40^o$: $\beta^- = 1, \beta^+ = 1000$

3. ELASTICITY EQUATION

We consider the elasticity equation with traction condition. Find $\mathbf{u} = (u_1, u_2)$ such that

$$\begin{aligned} -\nabla\cdot(\boldsymbol{\sigma}(\mathbf{u})) &= \mathbf{f} \text{ in } \Omega^s \quad (s=+,-) \\ \mathbf{u} &= 0 \text{ on } \partial\Omega \\ [\mathbf{u}]_\Gamma &= 0, \\ [\sigma(\mathbf{u})\cdot\mathbf{n}]_\Gamma &= 0 \text{ traction condition,} \end{aligned} \tag{3.1}$$

where $\sigma(\mathbf{u}) = 2\mu^s\epsilon(\mathbf{u}) + \lambda^s tr(\epsilon(\mathbf{u}))I$, $\epsilon(\mathbf{u}) = \frac{1}{2}(\nabla\mathbf{u} + \nabla\mathbf{u}^T)$, are stress tensor and deformation tensor, I the identity tensor.

Multiplying $\mathbf{v} \in (H_0^1(\Omega))^2$, applying Green's identity in each domain Ω^s, and summing over $s = +, -$ we have

$$a(\mathbf{u}, \mathbf{v}) = (\mathbf{f}, \mathbf{v}),$$

where

$$a(\mathbf{u}, \mathbf{v}) = \int_\Omega 2\mu\boldsymbol{\epsilon}(\mathbf{u}) : \boldsymbol{\epsilon}(\mathbf{v})dx + \int_\Omega \lambda \mathrm{div}\mathbf{u}\, \mathrm{div}\mathbf{v}\, dx,$$

the tensor inner product : is defined by

$$\boldsymbol{\epsilon}(\mathbf{u}) : \boldsymbol{\epsilon}(\mathbf{v}) = \sum_{i,j=1}^{2} \epsilon_{ij}(u)\epsilon_{ij}(v).$$

Difficulties with elasticity problems. Some difficulties in solving elasticity equations are

- The bilinear form $a(\mathbf{u}, \mathbf{v})$ is not coercive for certain FEM with Neumann or traction conditions.
- When the material's Poisson ratio approaches 1/2, the material becomes nearly incompressible and the so called "locking phenomena" occurs for low order standard nodal based methods.
- For the P_2 and P_3 conforming elements, the convergence orders tend to be suboptimal when the material is nearly incompressible.
- On the other hand, P_1/Q_1-nonconforming element can not be used since it fails to satisfy Korn's inequality [34].

Partial suggestions to overcome these difficulties are:

- Use nonconforming element of degree ≥ 2.
- The mixed methods can be applied to elasticity equations by introducing a new variable representing the divergence of the displacement.
- Use Kouhia and Stenberg(KS) [35] element which partially relaxes the continuity along the edges
- Use Hansbo and Larson [36] type P_1 nonconforming IFEM method with a stabilizing term (DG technique)

3.1. **CR-Immersed element for the elasticity interface problem.** We introduce an immersed element for elasticity equation with interface. Let us put

$$\hat{\boldsymbol{\phi}}_i(X) = \begin{cases} \hat{\boldsymbol{\phi}}_i^+(X) = \begin{pmatrix} a_0^+ + b_0^+ x + c_0^+ y, \\ a_1^+ + b_1^+ x + c_1^+ y, \end{pmatrix} & X = (x, y) \in T^+, \\ \hat{\boldsymbol{\phi}}_i^-(X) = \begin{pmatrix} a_0^- + b_0^- x + c_0^- y, \\ a_1^- + b_1^- x + c_1^- y, \end{pmatrix} & X = (x, y) \in T^- \end{cases}$$

We require that it satisfy

$$\begin{aligned}
\overline{\hat{\boldsymbol{\phi}}_i}|e_j &= \begin{cases} \delta_{ij} \\ 0 \end{cases}, \ j=1,2,3, \\
\overline{\hat{\boldsymbol{\phi}}_i}|e_j &= \begin{cases} 0 \\ \delta_{ij} \end{cases}, \ j=1,2,3, \\
[\hat{\boldsymbol{\phi}}_i](D) &= [\hat{\boldsymbol{\phi}}_i](E)=0, \quad \Big[\boldsymbol{\sigma}(\hat{\boldsymbol{\phi}}_i)\cdot\mathbf{n}\Big]_{\overline{DE}}=0.
\end{aligned}$$

The above equations yiels a determining system with matrix C

$$\begin{pmatrix}
0 & 0 & 0 & 1 & * & * & 0 & 0 & 0 & 0 & 0 & 0 \\
* & * & * & * & * & * & 0 & 0 & 0 & 0 & 0 & 0 \\
* & * & * & * & * & * & 0 & 0 & 0 & 0 & 0 & 0 \\
0 & 0 & 0 & 0 & 0 & 0 & 0 & 0 & 0 & 1 & * & * \\
0 & 0 & 0 & 0 & 0 & 0 & * & * & * & * & * & * \\
0 & 0 & 0 & 0 & 0 & 0 & * & * & * & * & * & * \\
1 & x^D & y^D & -1 & -x^D & -y^D & 0 & 0 & 0 & 0 & 0 & 0 \\
1 & x^E & y^E & -1 & -x^E & -y^E & 0 & 0 & 0 & 0 & 0 & 0 \\
0 & 0 & 0 & 0 & 0 & 0 & 1 & x^D & y^D & -1 & -x^D & -y^D \\
0 & 0 & 0 & 0 & 0 & 0 & 1 & x^E & y^E & -1 & -x^E & -y^E \\
0 & * & * & 0 & * & * & 0 & * & * & 0 & * & * \\
0 & * & * & 0 & * & * & 0 & * & * & 0 & * & *
\end{pmatrix}.$$

Proposition 3.1 (Uniqueness and existence of the element)**.** *The matrix C is invertible, hence the basis functions uniquely exist.*

Proof. See [6]. □

The immersed basis functions $\hat{\boldsymbol{\phi}}_i$, $i=1,\cdots,6$ are locally obtained by the degrees of freedom $v_i=(\delta_{1i},\delta_{2i},\delta_{3i},\delta_{4i},\delta_{5i},\delta_{6i},0,0,0,0,0,0)^T$. Such a (local) space is denoted by $\widehat{\mathbf{N}}(T)$. The global *immersed finite element space* $\widehat{\mathbf{N}}_h(\Omega)$ is the set of all functions $\phi\in(L_2(\Omega))^2$ such that

- $\boldsymbol{\phi}\in\widehat{\mathbf{N}}_h(T)$ if T is an interface element
- $\boldsymbol{\phi}\in\mathbf{N}_h(T)$ if T is not an interface element
- $\boldsymbol{\phi}$ vanishes on the boundary edges.

IFEM scheme for elasticity problems. Find $\mathbf{u}_h\in\widehat{\mathbf{N}}_h(\Omega)$ such that

$$a_h(\mathbf{u}_h,\mathbf{v}_h)=(\mathbf{f},\mathbf{v}_h),\ \forall\mathbf{v}_h\in\widehat{\mathbf{N}}_h(\Omega), \tag{3.2}$$

where

$$\begin{aligned} a_h(\mathbf{u}_h,\mathbf{v}_h): &= \sum_{T\in\mathcal{T}_h}\int_T 2\mu\boldsymbol{\epsilon}(\mathbf{u}_h):\boldsymbol{\epsilon}(\mathbf{v}_h)dx+\sum_{T\in\mathcal{T}_h}\int_T \lambda \mathrm{div}\mathbf{u}_h\,\mathrm{div}\mathbf{v}_h\,dx \\ &\quad +\tau\sum_{e\in\mathcal{E}}\int_e h^{-1}[\mathbf{u}_h][\mathbf{v}_h]ds \\ \|\mathbf{v}\|_{a_h}^2 &:= a_h(\mathbf{u}_h,\mathbf{v}_h). \end{aligned}$$

Lemma 3.2. *The form $a_h(\cdot,\cdot)$ is coercive.*

Proof. Need the following Korn type inequality [37]. With $Q(\mathbf{v}_h):=\mathbf{v}_h-\frac{1}{|T|}\int_T\mathbf{v}_h\,dx$

$$|\mathbf{v}_h|_{1,h}^2\le C\sum_{T\in\mathcal{T}_h}(\|\boldsymbol{\epsilon}(\mathbf{v}_h)\|_{0,T}^2+\|Q(\mathbf{v}_h)\|_{0,T}^2)+\sum_{e\in\mathcal{E}}\int_e\frac{\tau}{h}[\mathbf{v}_h]^2ds,\ \mathbf{v}_h\in\widehat{\mathbf{N}}(T),$$

$$\|Q(\mathbf{v}_h)\|_{0,T}^2 \le C(T)h|\mathbf{v}_h|_{1,T}^2.$$

Hence we have

$$|\mathbf{v}_h|_{1,h}^2\le C\sum_{T\in\mathcal{T}_h}\left(\|\boldsymbol{\epsilon}(\mathbf{v}_h)\|_{0,T}^2+\int_T\lambda|\mathrm{div}\mathbf{v}_h|^2dx\right)+\sum_{e\in\mathcal{E}}\int_e\frac{\tau}{h}[\mathbf{v}_h]^2ds \text{ for all } \mathbf{v}_h\in\widehat{\mathbf{N}}(T)$$

holds for all $\mathbf{v}_h\in\widehat{\mathbf{N}}(T)$ and for sufficiently small h. □

3.2. **Approximation Properties.** Define spaces $X(T)$ and $X_\Gamma(T)$:

$$\begin{aligned} X(T) &:= \left\{\mathbf{u}:\mathbf{u}\in(H^1(T))^2,\mathbf{u}\in(H^2(S))^2 \text{ for all } S=T_r^\pm,T^\pm\cap\Omega^\pm\right\} \\ X_\Gamma(T) &:= \left\{\mathbf{u}:\mathbf{u}\in X(T),\int_{\Gamma\cap T}(\boldsymbol{\sigma}(\mathbf{u})^- -\boldsymbol{\sigma}(\mathbf{u})^+)\cdot\mathbf{n}_\Gamma\,ds=0\right\} \end{aligned}$$

Note the relations

$$(\widetilde{H}^2(T))^2\hookrightarrow X(T)\hookrightarrow(H^1(T))^2$$
$$(\widetilde{H}^2_\Gamma(T))^2\cup\widehat{\mathbf{N}}_h(T)\hookrightarrow X_\Gamma(T)\hookrightarrow X(T)\hookrightarrow(H^1(T))^2$$

We introduce some norms.

$$\begin{aligned} \|\mathbf{u}\|_{b,m,T}^2 &= \|\mathbf{u}\|_{m,T}^2+m\cdot\|\sqrt{\lambda}\mathrm{div}\mathbf{u}\|_{0,T}^2,\ m=0,1 \\ |\mathbf{u}|_{X(T)}^2 &= |\mathbf{u}|_{2,T^-\cap\Omega^-}^2+|\mathbf{u}|_{2,T^+\cap\Omega^+}^2+|\mathbf{u}|_{2,T_r^-}^2+|\mathbf{u}|_{2,T_r^+}^2, \\ \|\mathbf{u}\|_{X(T)}^2 &= \|\mathbf{u}\|_{1,T}^2+|\mathbf{u}|_{X(T)}^2+\|\sqrt{\lambda}\mathrm{div}\mathbf{u}\|_{0,T}^2+\sum_{s=+,-}|\sqrt{\lambda}\mathrm{div}\mathbf{u}|_{1,T^s}^2 \\ |\!|\!|\mathbf{u}|\!|\!|_{2,T}^2 &= |\mathbf{u}|_{X(T)}^2+\sum_{s=+,-}|\sqrt{\lambda}\mathrm{div}\mathbf{u}|_{1,T^s}^2 \\ &\quad + \left|\int_{\Gamma\cap T}[\boldsymbol{\sigma}(\mathbf{u})\cdot\mathbf{n}_\Gamma]\,ds\right|^2+\sum_{i=1}^3|\overline{u_1}|_{e_i}|^2+\sum_{i=1}^3|\overline{u_2}|_{e_i}|^2, \end{aligned}$$

Lemma 3.3. *$|\!|\!| \cdot |\!|\!|_{2,T}$ is a norm on the space $X_\Gamma(T)$ which is equivalent to $\|\cdot\|_{X(T)}$.*

For any $\mathbf{u} \in (H^1(T))^2$, we define $I_h\mathbf{u} \in \widehat{\mathbf{N}}_h(T)$ by

$$\int_{e_i} I_h\mathbf{u}\, ds = \int_{e_i} \mathbf{u}\, ds,\ i = 1, 2, 3.$$

Now we are ready to prove the interpolation error estimate [6].

Theorem 3.1. *For any $\mathbf{u} \in (\widetilde{H}^2_\Gamma(\Omega))^2$, there exists a constant $C > 0$ such that for $m = 0, 1$*

$$\begin{aligned} \|\mathbf{u} - I_h\mathbf{u}\|_{m,h} + m \cdot \|\sqrt{\lambda}\mathrm{div}(\mathbf{u} - I_h\mathbf{u})\|_{L^2(\Omega)} &\leq Ch^{2-m}(\|\mathbf{u}\|_{\widetilde{H}^2(\Omega)} + m \cdot \sqrt{\lambda_M}\|\mathrm{div}\mathbf{u}\|_{\widetilde{H}^1(\Omega)}), \\ \|\mathbf{u} - I_h\mathbf{u}\|_{m,h} &\leq Ch^{2-m}\|\mathbf{u}\|_{\widetilde{H}^2(\Omega)}. \end{aligned}$$

Proof. Let $\check{T}$ be a reference interface element, $\check{\Gamma}$ be the corresponding local reference interface, and $\check{\mathbf{u}}(\check{\mathbf{x}}) := \mathbf{u} \circ \mathbf{F}(\check{\mathbf{x}})$, where $\mathbf{F} : \check{T} \to T$ denote the affine mapping to define the finite element in the real domain. Then for any $\check{\mathbf{u}} \in (\widetilde{H}^2_\Gamma(\check{T}))^2 \subset X_\Gamma(\check{T})$, (let us denote $\check{\mathbf{u}} = (\check{u}_1, \check{u}_2)$ and $I_h\check{\mathbf{u}} = (\check{w}_1, \check{w}_2)$)

$$\begin{aligned} |\!|\!|\check{\mathbf{u}} - I_h\check{\mathbf{u}}|\!|\!|^2_{2,\check{T}} &= |\check{\mathbf{u}} - I_h\check{\mathbf{u}}|^2_{X(\check{T})} + \sum_{s=+,-} |\sqrt{\lambda}\mathrm{div}(\check{\mathbf{u}} - I_h\check{\mathbf{u}})|^2_{1,\check{T}^s} \\ + \left| \int_{\check{\Gamma}\cap\check{T}} [(\boldsymbol{\sigma}(\check{\mathbf{u}}) - \boldsymbol{\sigma}(I_h\check{\mathbf{u}})) \cdot \mathbf{n}_\Gamma]\, ds \right|^2 &+ \sum_{i=1}^3 |(\overline{\check{u}_1 - \check{w}_1})|_{e_i}|^2 + \sum_{i=1}^3 |(\overline{\check{u}_2 - \check{w}_2})|_{e_i}|^2 \\ = |\check{\mathbf{u}} - I_h\check{\mathbf{u}}|^2_{X(\check{T})} + \sum_{s=+,-} |\sqrt{\lambda}\mathrm{div}(\check{\mathbf{u}} - I_h\check{\mathbf{u}})|^2_{1,\check{T}^s} &= |\check{\mathbf{u}}|^2_{X(\check{T})} + \sum_{s=+,-} |\sqrt{\lambda}\mathrm{div}\,\check{\mathbf{u}}|^2_{1,\check{T}^s}. \end{aligned}$$

Let $m = 0$ or 1. By Lemma 3.3 and scaling argument,

$$\begin{aligned} \|\mathbf{u} - I_h\mathbf{u}\|_{b,m,T} &\leq Ch^{1-m}\|\check{\mathbf{u}} - I_h\check{\mathbf{u}}\|_{b,m,\check{T}} \\ &\leq Ch^{1-m}\|\check{\mathbf{u}} - I_h\check{\mathbf{u}}\|_{X(\check{T})} \\ &\leq Ch^{1-m}|\!|\!|\check{\mathbf{u}} - I_h\check{\mathbf{u}}|\!|\!|_{2,\check{T}} \\ &= Ch^{1-m}(|\check{\mathbf{u}}|_{X(\check{T})} + m \cdot \sum_{s=+,-} |\sqrt{\lambda}\mathrm{div}\,\check{\mathbf{u}}|_{1,\check{T}^s}) \\ &\leq Ch^{2-m}(|\mathbf{u}|_{X(T)} + m \cdot \sum_{s=+,-} |\sqrt{\lambda}\mathrm{div}\,\mathbf{u}|_{1,T^s}) \\ &\leq Ch^{2-m}(\|\mathbf{u}\|_{\widetilde{H}^2(T)} + m \cdot \sum_{s=+,-} |\sqrt{\lambda}\mathrm{div}\,\mathbf{u}|_{1,T^s}). \end{aligned}$$

For the second assertion one can proceed exactly the same way without the terms involving $\mathrm{div}\mathbf{u}$ in the definition of norms $\|\cdot\|_{b,m,T}$, $\|\cdot\|_{X(T)}$ and $|\!|\!|\cdot|\!|\!|_{2,T}$ to obtain the desired estimate. □

3.3. **Consistency error estimate.** The scheme is not consistent in sense that

$$a_h(\mathbf{u},\mathbf{v}_h)-a_h(\mathbf{u}_h,\mathbf{v}_h)=\sum_{T\in\mathcal{T}_h}\int_{\partial T}\boldsymbol{\sigma}(\mathbf{u})\mathbf{n}\cdot\mathbf{v}_h ds.$$

Hence we need to estimate the following term

$$\sum_{T\in\mathcal{T}_h}\int_{\partial T}\boldsymbol{\sigma}(\mathbf{u})\mathbf{n}\cdot\mathbf{v}_h ds.$$

We have

$$\begin{aligned}
\sum_{T\in\mathcal{T}_h}\int_{\partial T}\boldsymbol{\sigma}(\mathbf{u})\mathbf{n}\cdot\mathbf{v}_h ds &= \sum_{T\in\mathcal{T}_h}\sum_{e\subset\partial T}\int_e\boldsymbol{\sigma}(\mathbf{u})\mathbf{n}\cdot[\mathbf{v}_h]ds\\
&= \sum_{e\in\mathcal{E}}\int_e(\boldsymbol{\sigma}(\mathbf{u})\cdot\mathbf{n}-\overline{\boldsymbol{\sigma}(\mathbf{u})\cdot\mathbf{n}})\cdot[\mathbf{v}_h]ds\\
&\le \sum_{T\in\mathcal{T}_h}Ch\|\boldsymbol{\sigma}(\mathbf{u})\|_{1,T}|\mathbf{v}_h|_{1,T}\\
&= \sum_{T\in\mathcal{T}_h}Ch\|2\mu\boldsymbol{\epsilon}(\mathbf{u})+\lambda\mathrm{div}\mathbf{u}\cdot\boldsymbol{\delta}\|_{1,T}|\mathbf{v}_h|_{1,T}\\
&\le \sum_{T\in\mathcal{T}_h}Ch(\|2\mu\boldsymbol{\epsilon}(\mathbf{u})\|_{1,T}+\|\lambda\mathrm{div}\mathbf{u}\|_{1,T})|\mathbf{v}_h|_{1,T}\\
&\le \sum_{T\in\mathcal{T}_h}Ch(2\mu\|\mathbf{u}\|_{2,T}+\lambda\|\mathrm{div}\mathbf{u}\|_{1,T})\|\mathbf{v}_h\|_{a,h},
\end{aligned}$$

under the assumption that $\boldsymbol{\sigma}(\mathbf{u})\in\mathbf{H}^1(T)$.

3.4. **Consistent Scheme.** A drawback of the previous scheme might be a high regularity assumption that $\boldsymbol{\sigma}(\mathbf{u})\in\mathbf{H}^1(T)$. To avoid such a regularity assumption, we may consider a consistent scheme as follows.

$$\begin{aligned}
a_h^c(\mathbf{u}_h,\mathbf{v}_h):=&\sum_{T\in\mathcal{T}_h}\left(\int_T 2\mu\boldsymbol{\epsilon}(\mathbf{u}):\boldsymbol{\epsilon}(\mathbf{v})dx+\int_T\lambda\mathrm{div}\mathbf{u}\,\mathrm{div}\mathbf{v}\,dx\right)+\sum_{e\in\mathcal{E}}\int_e\frac{\tau}{h}[\mathbf{u}][\mathbf{v}]ds\\
&-\sum_{e\in\mathcal{E}}\int_e\{\boldsymbol{\sigma}(\mathbf{u})\cdot\mathbf{n}\}\cdot[\mathbf{v}]ds-\epsilon\sum_{e\in\mathcal{E}}\int_e\{\boldsymbol{\sigma}(\mathbf{v})\cdot\mathbf{n}\}\cdot[\mathbf{u}]ds,\ \forall\mathbf{u},\mathbf{v}\in\mathbf{H}_h(\Omega). \quad (3.3)
\end{aligned}$$

Define

$$\begin{aligned}
\|\mathbf{v}\|_{a_h^c}^2 &:= \sum_{T\in\mathcal{T}_h}\|\mathbf{v}\|_{a,T}^2+\sum_{e\in\mathcal{E}}\left(\int_e h|\{\boldsymbol{\sigma}(\mathbf{v})\cdot\mathbf{n}\}|^2ds+\int_e\frac{\tau}{h}[\mathbf{v}]^2ds\right),\\
\|\mathbf{v}\|_{a,T}^2 &:= \int_T 2\mu\epsilon(\mathbf{v}):\epsilon(\mathbf{v})dx+\int_T\lambda|\mathrm{div}\mathbf{v}|^2dx.
\end{aligned}$$

Then we have

Lemma 3.4. *There exist positive constants C_0 and C_1 such that the following inequalities hold.*

$$\begin{aligned} a_h^c(\mathbf{u},\mathbf{v}) &\leq C_0\|\mathbf{u}\|_{a_h^c}\|\mathbf{v}\|_{a_h^c},\ \forall \mathbf{u},\mathbf{v}\in \mathbf{H}_h(\Omega), \\ C_1\|\mathbf{v}_h\|_{a_h^c}^2 &\leq a_h^c(\mathbf{v}_h,\mathbf{v}_h),\ \forall \mathbf{v}_h\in \hat{\mathbf{N}}_h(\Omega). \end{aligned}$$

3.5. **Main results.** For both inconsistent and consistent scheme, we have

Theorem 3.5. *Let $\mathbf{u}$ (resp. $\mathbf{u}_h$) be the solution of (3.1)(reps. (3.2) or (3.3)). Then we have*

$$\|\mathbf{u}-\mathbf{u}_h\|_{a_h} \leq Ch(\|\mathbf{u}\|_{\widetilde{H}^2(\Omega)} + \lambda_M\|\mathrm{div}\mathbf{u}\|_{\widetilde{H}^1(\Omega)}).$$

3.6. **Numerical results for elasticity problem.**

Example 3.6. *Let the exact solution be $u = \left(\frac{1}{\mu}\left(x^2+y^2-r_0^2\right)x, \frac{1}{\mu}\left(x^2+y^2-r_0^2\right)y\right)$ and the interface be given by $x^2+y^2-r_0^2=0$.*

$1/h$	$\|\mathbf{u}-\mathbf{u}_h\|_0$	*order*	$\|\mathrm{div}\mathbf{u}-\mathrm{div}\mathbf{u}_h\|_0$	*order*	$\|\mathbf{u}-\mathbf{u}_h\|_{1,h}$	*order*
8	*2.910e-3*		*7.972e-2*		*8.598e-2*	
16	*7.450e-4*	*1.966*	*3.822e-2*	*1.061*	*4.155e-2*	*1.049*
32	*1.841e-4*	*2.017*	*1.942e-2*	*0.977*	*2.091e-2*	*0.991*
64	*4.606e-5*	*1.999*	*9.787e-3*	*0.989*	*1.049e-2*	*0.996*
128	*1.143e-5*	*2.010*	*4.920e-3*	*0.992*	*5.255e-3*	*0.997*
256	*2.851e-6*	*2.004*	*2.466e-3*	*0.997*	*2.630e-3*	*0.999*

TABLE 6. $\mu^- = 1,\ \mu^+ = 10, \lambda = 5\mu, r_0 = 0.48$ (Example 3.6).

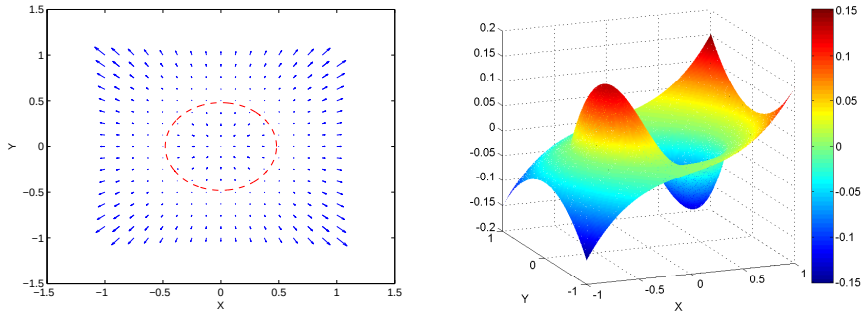

FIGURE 6. Left figure shows the vector fields and right figure shows the x-component. $\mu^- = 1,\ \mu^+ = 10, \lambda = 5\mu, r_0 = 0.48$ (Example 3.6).

Example 3.7. *The exact solution is $u = \left(\frac{1}{\mu}\left(\frac{x^2}{4}+y^2-r_0^2\right)x, \frac{1}{\mu}\left(\frac{x^2}{4}+y^2-r_0^2\right)y\right)$ with interface $\frac{x^2}{4}+y^2-r_0^2=0$.*

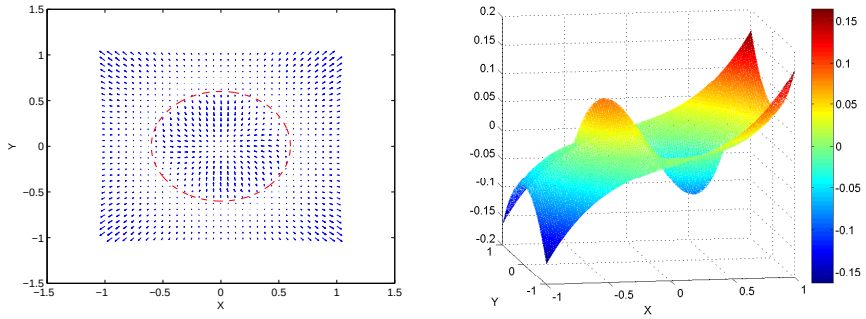

FIGURE 7. Left figure shows the vector fields and right figure shows the x-component. $\mu^- = 1,\ \mu^+ = 10, \lambda = 1000\mu, \nu = 0.4995, r_0 = 0.6$ (Example 3.7).

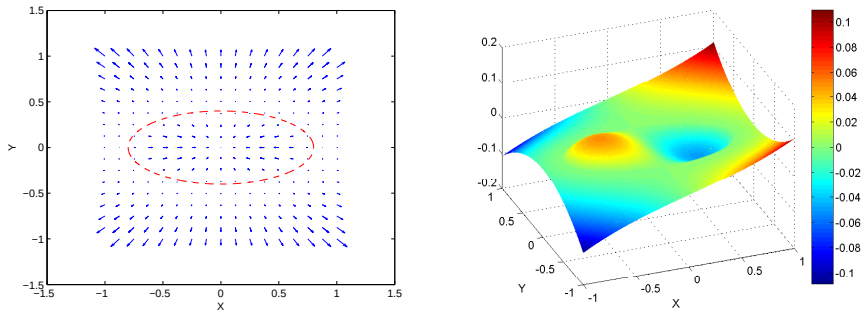

FIGURE 8. Left figure shows the vector fields and right figure shows the x-component. $\mu^- = 1,\ \mu^+ = 10, \lambda = 5\mu, r_0 = 0.4$, (Example 3.7).

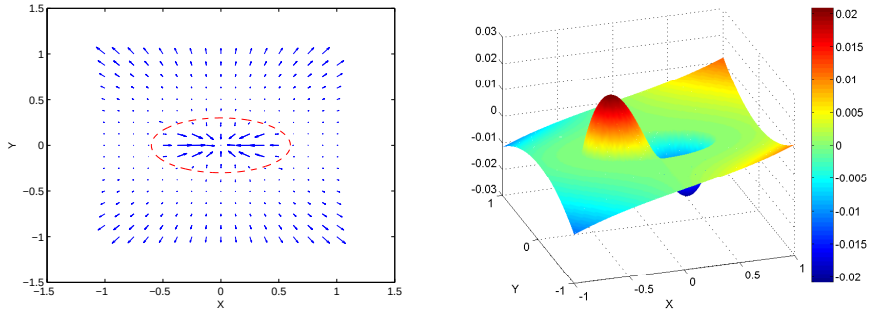

FIGURE 9. Left figure shows the vector fields and right figure shows the x-component. $\mu^- = 1,\ \mu^+ = 100, \lambda = 5\mu, r_0 = 0.3$, (Example 3.7).

$1/h$	$\|\mathbf{u}-\mathbf{u}_h\|_0$	*order*	$\|\mathrm{div}\mathbf{u}-\mathrm{div}\mathbf{u}_h\|_0$	*order*	$\|\mathbf{u}-\mathbf{u}_h\|_{1,h}$	*order*
8	*7.655e-2*		*1.125e-1*		*1.628e-0*	
16	*2.372e-2*	*1.690*	*5.570e-2*	*1.014*	*9.065e-1*	*0.846*
32	*6.806e-2*	*1.801*	*2.829e-2*	*0.978*	*4.518e-1*	*1.004*
64	*1.847e-3*	*1.882*	*1.417e-2*	*0.997*	*2.247e-1*	*1.008*
128	*4.811e-4*	*1.941*	*7.110e-3*	*0.995*	*1.111e-1*	*1.016*
256	*1.230e-4*	*1.968*	*3.563e-3*	*0.997*	*5.534e-2*	*1.006*

TABLE 7. $\mu^- = 1,\ \mu^+ = 10, \lambda = 1000\mu, \nu = 0.4995, r_0 = 0.6$ (Example 3.7 - nearly incompressible case).

$1/h$	$\|\mathbf{u}-\mathbf{u}_h\|_0$	order	$\|\mathrm{div}\mathbf{u}-\mathrm{div}\mathbf{u}_h\|_0$	order	$\|\mathbf{u}-\mathbf{u}_h\|_{1,h}$	order
8	2.477e-3		5.920e-2		6.744e-2	
16	6.689e-4	1.888	2.909e-2	1.025	3.340e-2	1.014
32	1.704e-4	1.973	1.480e-2	0.975	1.694e-2	0.979
64	4.200e-5	2.020	7.485e-3	0.983	8.531e-3	0.990
128	1.029e-5	2.029	3.765e-3	0.992	4.281e-3	0.995
256	2.579e-6	1.996	1.886e-3	0.997	2.144e-3	0.998

TABLE 8. $\mu^- = 1,\ \mu^+ = 10, \lambda = 5\mu, r_0 = 0.4$, (Example 3.7).

$1/h$	$\|\mathbf{u}-\mathbf{u}_h\|_0$	order	$\|\mathrm{div}\mathbf{u}-\mathrm{div}\mathbf{u}_h\|_0$	order	$\|\mathbf{u}-\mathbf{u}_h\|_{1,h}$	order
8	2.018e-3		3.164e-2		3.788e-2	
16	6.644e-4	1.647	1.424e-2	1.151	2.066e-2	0.875
32	1.376e-4	2.227	7.314e-3	0.962	9.592e-3	1.107
64	2.736e-5	2.330	3.735e-3	0.969	4.458e-3	1.105
128	6.896e-6	1.988	1.880e-3	0.991	2.229e-3	1.000
256	1.726e-6	1.998	9.434e-4	0.994	1.107e-3	1.010

TABLE 9. $\mu^- = 1,\ \mu^+ = 100, \lambda = 5\mu, r_0 = 0.3$, (Example 3.7).

4. MULTIGRID ALGORITHMS

The IFEM may not be meaningful without the applicability of multigrid algorithms. Multigrid algorithms were first introduced in [38], and have been known to be very efficient for many class of FEM discretization [39, 40] and their convergence behaviors were discussed in [41, 39, 40, 42, 43, 44, 45] and references therein. Multigrid algorithms for IFEM were first introduced in [46] and analyzed in [47]. We describe them in this section.

4.1. **Multigrid algorithms for Lagrangian based IFEM spaces.** For simplicity,we describe multigrid algorithms for Lagrangian based IFEM space only. The multigrid algorithms for Crouzeix-Raviart nonconforming element based IFEM can be described similarly.

Let $\mathcal{T}_{h_k}$, $k = 0, ..., J$ be hierarchical triangulations of Ω with mesh size $h_k = 2^{-k}h_0$, where h_0 is the meshsize of the coarsest grid. For simplicity, we replace the subscript h_k simply by the subscript k. For example,

$$\mathcal{T}_k = \mathcal{T}_{h_k},\ a_k(\cdot,\cdot) = a_{h_k}(\cdot,\cdot),\ \widehat{S}_k(\Omega) = \widehat{S}_{h_k}(\Omega).$$

We let A_k be the matrix arising from the linear system obtained from (2.5).

Since the IFEM spaces are not nested, i.e.,

$$\widehat{S}_1 \not\subseteq \widehat{S}_2 \not\subseteq \cdots \not\subseteq \widehat{S}_J,$$

it is important to construct an efficient prolongation operator. We define a prolongation operator $\widehat{I}_k : \widehat{S}_{k-1}(\Omega) \to \widehat{S}_k(\Omega)$ so that the prolongated functions satisfy the local flux condition on the fine space.

On a non-interface element, $\widehat{I}_k$ is defined as the same as usual prolongation operator for node based FEM. Now to define $\widehat{I}_k$ on interface elements, suppose that $T_1 = \triangle X_1X_2X_3$ and $T_2 = \triangle X_1X_4X_3$ are tow adjacent interface elements in $\mathcal{T}_{k-1}$ (See Figure 10). Given a function $v \in \widehat{S}_{k-1}(\Omega)$ it suffices to define node values of $\widehat{I}_k(v)$ at $X_1, X_2, ..., X_9$. Firstly, $\widehat{I}_k(v)(X)$ is defined by $v(X)$ where X are nodes on coarse triangle, i.e., $X = X_1, X_2, X_3, X_4$. Now consider the mid points of vertices $X_5, X_6, \ldots, X_9$ as in Figure 10. However, we will describe $\widehat{I}_k(v)(X)$ for the mid points X of vertices. We consider X_5. We define $\widehat{I}_k v(X_5)$ is defined as the average values:

$$\widehat{I}_k v(X_5) = \frac{1}{2}\left(v_1^-(X_5) + v_2^-(X_5)\right),$$

where $v_1^- = v_1|_{T_1^-}$ and $v_2^- = v_2|_{T_2^-}$. The values of $\widehat{I}_k v(X)$ at $X = X_6, X_7, X_8, X_9$ are defined similarly.

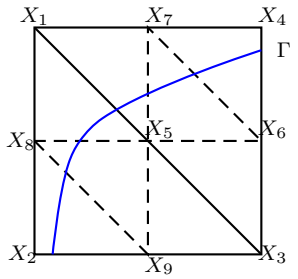

FIGURE 10. $\triangle X_1X_2X_3$ abd $\triangle X_1X_4X_3$ are interface triangles in $\mathcal{T}_{k-1}$ and sub triangles are elements in $\mathcal{T}_k$. The blue curve represents the interface Γ.

We summarize the description of prolongation operator. If $v \in \widehat{S}_{k-1}(\Omega)$, then $\widehat{I}_k v \in \widehat{S}_k(\Omega)$ is defined by

$$\widehat{I}_k v(X) = \begin{cases} v(X) & \text{if } X \text{ if is node of } \mathcal{T}_{k-1}, \\ \frac{1}{2}\left(v|_{T_1}(X) + v|_{T_2}(X)\right) & \text{if } X \text{ is a midpoint of an edge } e \text{ shared} \\ & \text{by two triangles } T_1,\ T_2 \in \mathcal{T}_{k-1}. \end{cases}$$

Next, we define the restriction operator P_{k-1}^0 as the adjoint operators of $\widehat{I}_k$ with respect to $(\cdot,\cdot)_k$, i.e., P_{k-1}^0 to satisfy: for $u \in \widehat{S}_{k-1}(\Omega)$ and $\phi \in \widehat{S}_k(\Omega)$,

$$(P_{k-1}^0 u, \phi)_{k-1} = (u, \widehat{I}_k \phi)_k.$$

Here, $(\cdot,\cdot)_k$ is defined by

$$(u_k, v_k)_k = \sum_{T \in \mathcal{T}_k} \int_T u_k v_k.$$

Lastly, we define smoothing operator R_k which can be Gauss-Seidel or Jacobi or any other smoothing operators. To define symmetric multigrid algorithm, we define adjoint smoothing operator R_k^t.

Now we are ready to describe multigrid operator $B_k : \widehat{S}_k(\Omega) \to \widehat{S}_k(\Omega)$ recursively for $k = 1, 2, \ldots, J$.

Algorithm B_k.

Set $B_0 g_0 = A_0^{-1} g_0$. Suppose B_{k-1} is defined.

We define $B_k g_k$ as follows.

1. Set $x^0 = 0$ and $q^0 = 0$
2. Define x^i for $i = 1, ..., m(k)$ by

$$x^i = x^{i-1} + R_k(g_k - A_k x^{i-1})$$

3. Define $y^{m(k)}$ by $y^{m(k)} = x^{m(k)} + \widehat{I}_k q^p$ where q^j for $j = 1, ..., p$ is defined by

$$q^j = q^{j-1} + B_{k-1}[P_{k-1}^0(g_k - A_k x^m) - A_{k-1} q^{j-1}]$$

4. Define y^i for $i = m(k)+1, ..., 2m(k)$ by

$$y^i = y^{i-1} + R_k^t(g_k - A_k y^{i-1})$$

5. Set $B_k g_k = y^{2m(k)}$.

We note that the B_k is a symmetric operator. The algorithm is similar to conventional multigrid methods for FEM, but we have used the modified prolongation operator which plays an important role in the convergence of the algorithm. When $p = 1$, the algorithm is corresponds to $\mathcal{V}$-cycle and the case of $p = 2$ corresponds to $\mathcal{W}$-cycle.

4.2. **Convergence analysis of MG.** We remark that the discretized spaces at level $k, k = 1, \cdots, J$ are not nested. The general frameworks for the convergence analysis of the multigrid algorithms on the non-nested spaces are given by Bramble et al. in [44]. We need some assumptions. Here, λ_k is the largest eigenvalue of A_k.

(A.1) **Smoothing property**. There exists a constant $C_R > 0$ such that for all $u \in \widehat{S}_k(\Omega)$,

$$\frac{\|u\|_k^2}{\lambda_k} \leq C_R(\tilde{R}_k u, u)_k,$$

where $\tilde{R}_k = (I - K_k^* K_k)A_k^{-1}$, $K_k = I - R_k A_k$ and $K_k^* = I - R_k^t A_k$.

(A.2) There exists a constant C^*, such that

$$A_k(\widehat{I}_k u, \widehat{I}_k u) \leq C^* A_{k-1}(u, u), \quad \forall u \in \widehat{S}_{k-1}(\Omega).$$

(A.3) **Regularity and approximation** For some $0 < \alpha \leq 1$, there exists a constant $C_\alpha > 0$ such that

$$|a_k((I - \widehat{I}_k P_{k-1})u, u)| \leq C_\alpha \left(\frac{\|A_k u\|_k^2}{\lambda_k}\right)^\alpha a_k(u, u)^{1-\alpha}.$$

for all $u \in \widehat{S}_k(\Omega)$.

The following theorem is given in [44].

Theorem 4.1. *Suppose $p = 2$ and $m(k) = m$ for all k in the algorithm. Assume (A.1), (A.2) and (A.3) hold. If "m is sufficiently large", then we have*

$$|a_k((I - B_k A_k)u, u)| \leq \delta a_k(u, u) \quad \forall u \in \widehat{S}_k(\Omega),$$

where

$$\delta = \frac{M}{M + m^\alpha}$$

for some positive constant $M > 0$.

Let us examine the assumptions (A.1). By the definition of the bilinear form in (2.5), A_k is symmetric and positive definite. Moreover, A_k is sparse since the basis function in $\widehat{S}_k(\Omega)$ has support in less than 6 elements. Thus, the standard operators such as Gasuss-Seidel or Jacobi satisfy (A.1) (see [48]).

The assumptions (A.2)-(A.3) are proved in [47], rigorously, which together with (A.1) lead to the conclusion that the $\mathcal{W}$-cycles are contracting.

4.3. **Numerical results.**

Example 4.1. *The interface is given by $\Gamma = \{(x, y) : y - 3x(x - 0.3)(x - 0.8) - 0.38 = 0\}$ and the coefficient is $\beta^- = 1, \beta^+ = 1000$. The exact solution $u(x, y)$ is*

$$u(x, y) = \begin{cases} (y - 3x(x - 0.3)(x - 0.8) - 0.38)/\beta^- & \text{if } (x, y) \in \Omega^-, \\ \\ (y - 3x(x - 0.3)(x - 0.8) - 0.38)/\beta^+ & \text{if } (x, y) \in \Omega^+. \end{cases}$$

We use $\mathcal{V}$-cycle ($p = 1$) with only one pre and post smoothing for the multigrid solver. We report the number of iterations and convergence rates in Table 10. We observe the number of iterations are bounded for all levels.

We compare the CPU time of the $\mathcal{V}$-cycle with the CG and the diagonally preconditioned CG (D-PCG) in Table 11. The CPU time of $\mathcal{V}$-cycle grows like $\mathcal{O}(N)$ while the CPU times of CG and D-PCG grows like $\mathcal{O}(N^{3/2})$, where N is the number of the unknowns.

	$\mathcal{V}(1,1)$-*cycle*	
$1/h_J$	*Iter.*	*ratio*
32	*38*	*0.693*
64	*39*	*0.701*
128	*27*	*0.598*
256	*25*	*0.575*

TABLE 10. The number of iterations and convergence rates of $\mathcal{V}(1,1)$-cycle for $\widehat{S}_J(\Omega)$ for Example 4.1.

$1/h_J$	$\mathcal{V}(1,1)$-*cycle*	*CG*	*D-PCG*
32	*0.748*	*4.977*	*0.296*
64	*1.763*	*58.874*	*2.247*
128	*3.370*	*455.399*	*17.581*
256	*10.857*	*3628.578*	*132.616*

TABLE 11. CPU time of various solvers for $\widehat{S}_J(\Omega)$ for Example 4.1.

REFERENCES

[1] Z. LI, T. LIN, AND X. WU, *New cartesian grid methods for interface problems using the finite element formulation*, Numerische Mathematik, 96 (2003), pp. 61–98.

[2] Z. LI, T. LIN, Y. LIN, AND R. C. ROGERS, *An immersed finite element space and its approximation capability*, Numerical Methods for Partial Differential Equations, 20 (2004), pp. 338–367.

[3] H. JI, J. CHEN, AND Z. LI, *A symmetric and consistent immersed finite element method for interface problems*, Journal of Scientific Computing, 61 (2014), pp. 533–557.

[4] T. LIN, Y. LIN, AND X. ZHANG, *Partially penalized immersed finite element methods for elliptic interface problems*, SIAM Journal on Numerical Analysis, 53 (2015), pp. 1121–1144.

[5] D. Y. KWAK AND J. LEE, *A modified P_1-immersed finite element method*, International Journal of Pure and Applied Mathematics, 104 (2015), pp. 471–494.

[6] D. Y. KWAK, S. JIN, AND D. KYEONG, *A stabilized P_1-nonconforming immersed finite element method for the interface elasticity problems*, ESAIM: Mathematical Modelling and Numerical Analysis, 51 (2017), pp. 187–207.

[7] I. BABUŠKA, *The finite element method for elliptic equations with discontinuous coefficients*, Computing, 5 (1970), pp. 207–213.

[8] T. BELYTSCHKO, C. PARIMI, N. MOËS, N. SUKUMAR, AND S. USUI, *Structured extended finite element methods for solids defined by implicit surfaces*, International journal for Numerical Methods in Engineering, 56 (2003), pp. 609–635.
[9] T. BELYTSCHKO AND T. BLACK, *Elastic crack growth in finite elements with minimal remeshing*, International Journal for Numerical Methods in Engineering, 45 (1999), pp. 601–620.
[10] P. KRYSL AND T. BELYTSCHKO, *An efficient linear-precision partition of unity basis for unstructured meshless methods*, Communications in Numerical Methods in Engineering, 16 (2000), pp. 239–255.
[11] G. LEGRAIN, N. MOES, AND E. VERRON, *Stress analysis around crack tips in finite strain problems using the extended finite element method*, International Journal for Numerical Methods in Engineering, 63 (2005), pp. 290–314.
[12] N. MOËS, J. DOLBOW, AND T. BELYTSCHKO, *A finite element method for crack growth without remeshing*, International journal for numerical methods in engineering, 46 (1999), pp. 131–150.
[13] M. CROUZEIX AND P.-A. RAVIART, *Conforming and nonconforming finite element methods for solving the stationary stokes equations I*, Revue Française D'automatique Informatique Recherche Opérationnelle. Mathématique, 7 (1973), pp. 33–75.
[14] D. Y. KWAK, K. T. WEE, AND K. S. CHANG, *An analysis of a broken P_1-nonconforming finite element method for interface problems*, SIAM Journal on Numerical Analysis, 48 (2010), pp. 2117–2134.
[15] S. H. CHOU, D. Y. KWAK, AND K. T. WEE, *Optimal convergence analysis of an immersed interface finite element method*, Advances in Computational Mathematics, 33 (2010), pp. 149–168.
[16] D. N. ARNOLD, *An interior penalty finite element method with discontinuous elements*, SIAM journal on Numerical Analysis, 19 (1982), pp. 742–760.
[17] D. N. ARNOLD, F. BREZZI, B. COCKBURN, AND D. MARINI, *Discontinuous Galerkin methods for elliptic problems*, in Discontinuous Galerkin Methods, Springer, 2000, pp. 89–101.
[18] C. DAWSON, S. SUN, AND M. F. WHEELER, *Compatible algorithms for coupled flow and transport*, Computer Methods in Applied Mechanics and Engineering, 193 (2004), pp. 2565–2580.
[19] K. S. CHANG AND D. Y. KWAK, *Discontinuous bubble scheme for elliptic problems with jumps in the solution*, Computer Methods in Applied Mechanics and Engineering, 200 (2011), pp. 494–508.
[20] I. K. GWANGHYUN JO, DO Y. KWAK, *Two discontinuous bubble schemes for elliptic interface problems with jumps*, preprint.
[21] T. LIN AND X. ZHANG, *Linear and bilinear immersed finite elements for planar elasticity interface problems*, Journal of Computational and Applied Mathematics, 236 (2012), pp. 4681–4699.
[22] T. LIN, D. SHEEN, AND X. ZHANG, *A locking-free immersed finite element method for planar elasticity interface problems*, Journal of Computational Physics, 247 (2013), pp. 228–247.
[23] J. H. BRAMBLE AND J. T. KING, *A finite element method for interface problems in domains with smooth boundaries and interfaces*, Advances in Computational Mathematics, 6 (1996), pp. 109–138.
[24] Z. CHEN AND J. ZOU, *Finite element methods and their convergence for elliptic and parabolic interface problems*, Numerische Mathematik, 79 (1998), pp. 175–202.
[25] J. DOUGLAS AND T. DUPONT, *Interior penalty procedures for elliptic and parabolic galerkin methods*, in Computing methods in applied sciences, Springer, 1976, pp. 207–216.
[26] C. E. BAUMANN AND J. T. ODEN, *A discontinuous hp finite element method for convectiondiffusion problems*, Computer Methods in Applied Mechanics and Engineering, 175 (1999), pp. 311–341.
[27] S. H. CHOU, D. Y. KWAK, AND K. Y. KIM, *Mixed finite volume methods on nonstaggered quadrilateral grids for elliptic problems*, Mathematics of Computation, 72 (2003), pp. 525–539.
[28] S.-H. CHOU AND S. TANG, *Conservative P_1 conforming and nonconforming Galerkin fems: effective flux evaluation via a nonmixed method approach*, SIAM Journal on Numerical Analysis, 38 (2000), pp. 660–680.
[29] B. COURBET AND J. CROISILLE, *Finite volume box schemes on triangular meshes*, ESAIM: Mathematical Modelling and Numerical Analysis, 32 (1998), pp. 631–649.
[30] F. BREZZI, J. DOUGLAS JR, AND L. D. MARINI, *Two families of mixed finite elements for second order elliptic problems*, Numerische Mathematik, 47 (1985), pp. 217–235.

[31] F. BREZZI AND M. FORTIN, *Mixed and hybrid finite element methods*, vol. 15, Springer-Verlag, New York, 1991.
[32] P. A. RAVIART AND J. M. THOMAS, *A mixed finite element method for 2-nd order elliptic problems*, Mathematical aspects of finite element methods, (1977), pp. 292–315.
[33] D. N. ARNOLD AND F. BREZZI, *Mixed and nonconforming finite element methods: implementation, postprocessing and error estimates*, ESAIM: Mathematical Modelling and Numerical Analysis, 19 (1985), pp. 7–32.
[34] R. S. FALK, *Nonconforming finite element methods for the equations of linear elasticity*, Mathematics of Computation, 57 (1991), pp. 529–550.
[35] R. KOUHIA AND R. STENBERG, *A linear nonconforming finite element method for nearly incompressible elasticity and stokes flow*, Computer Methods in Applied Mechanics and Engineering, 124 (1995), pp. 195–212.
[36] P. HANSBO AND M. G. LARSON, *Discontinuous Galerkin and the Crouzeix–Raviart element: application to elasticity*, ESAIM: Mathematical Modelling and Numerical Analysis, 37 (2003), pp. 63–72.
[37] S. C. BRENNER, *Korn's inequalities for piecewise H_1 vector fields*, Mathematics of Computation, (2004), pp. 1067–1087.
[38] R. FEDORENKO, *The speed of convergence of one iterative process*, USSR Computational Mathematics and Mathematical Physics, 4 (1964), pp. 559–564.
[39] W. HACKBUSCH, *Multi-grid methods and applications*, vol. 4, Springer-Verlag, Berlin, 1985.
[40] S. F. MCCORMICK, *Multigrid methods*, vol. 3, SIAM, 1987.
[41] R. NICOLAIDES, *On some theoretical and practical aspects of multigrid methods*, Mathematics of Computation, 33 (1979), pp. 933–952.
[42] J. H. BRAMBLE AND J. E. PASCIAK, *New convergence estimates for multigrid algorithms*, Mathematics of Computation, 49 (1987), pp. 311–329.
[43] S. C. BRENNER, *An optimal-order multigrid method for P_1 nonconforming finite elements*, mathematics of computation, 52 (1989), pp. 1–15.
[44] J. H. BRAMBLE, J. E. PASCIAK, AND J. XU, *The analysis of multigrid algorithms with nonnested spaces or noninherited quadratic forms*, Mathematics of Computation, 56 (1991), pp. 1–34.
[45] D. BRAESS, W. DAHMEN, AND C. WIENERS, *A multigrid algorithm for the mortar finite element method*, SIAM Journal on Numerical Analysis, 37 (1999), pp. 48–69.
[46] G. JO AND D. Y. KWAK, *An IMPES scheme for a two-phase flow in heterogeneous porous media using a structured grid*, Computer Methods in Applied Mechanics and Engineering, (2017).
[47] D. Y. K. GWANGHYUN JO, *Geometric multigrid algorithms for elliptic interface problems using structured grids*, Numerical Algorithms, (2018).
[48] J. H. BRAMBLE AND J. E. PASCIAK *The analysis of smoothers for multigrid algorithms*, Mathematics of Computation, 58 (1992), pp. 467–488.